Journal of Life Sciences *JoLS*
Vol. 3, No. 1, March 2021 *www.JournalofLifeSciences.Org*

In silico screening for investigating the potential activity of phytoligands against SARS-CoV-2

Acharya Balkrishna[1,2], Pallavi Thakur[1], Shivam Singh[1], Namita Singh[3], Ankit Tanwar[4]*, Rakesh Kumar Sharma[5*]

[1] Drug Discovery and Development Division, Patanjali Research Institute, Haridwar, India
[2] Department of Allied and Applied Sciences, University of Patanjali, Haridwar, India
[3] Guru Jambheshwar University of Science and Technology, Hisar, Haryana, India
[4]Department of Cell Biology, Albert Einstein College of Medicine, New York, USA
[5] Saveetha Institute of Medical and Technical Sciences, 162, Poonamallee High Road, Chennai, India

*** Correspondence:**

1. Prof. (Dr.) Rakesh Kumar Sharma, Vice-Chancellor, Saveetha Institute of Medical and Technical Sciences, and Ex-Director, DFRL, DRDO, Ministry of Defence, India, Email Id: rksharmadrl@yahoo.com;

2. Ankit Tanwar, Scientist, Department of Cell Biology, Albert Einstein College of Medicine, New York, NY, 10461, USA; E-mail: tanwar.ankit9@gmail.com

Abstract:

SARS-CoV-2 causes COVID-19, a life-threatening respiratory illness with high rates of morbidity and mortality. As of date, there is no specific medicine to treat COVID-19. Therefore, there is an acute need to identify evidence-based holistic and safe mitigators. The present study aims to screen phytochemicals based on bioprospection analysis and subsequently predicting their binding potential to SARS-CoV-2 proteins *in silico*. The drug likeliness and ADMETox descriptors of 24 phytoligands were computationally predicted. Docking studies were further conducted with those phytoligands that qualified the drug likeliness parameters. Docking studies suggested that the herbal moiety, namely, gamma-glutamyl-S-allylcysteine demonstrated highly significant binding energies with viral spike glycoprotein, endoribonuclease, and main protease (binding energy ≥ -490 kcal/mol for all the tested target viral proteins). Gamma-glutamyl-S-allylcysteine demonstrated more significant binding potential as compared to the known chemical analog, *i.e.*, hydroxychloroquine, as observed in the computational docking studies. This study serves to present pre-eminent information for further clinical studies highlighting the utility of herbal ligands as probable lead molecules for mitigating novel Coronavirus infection.

Keywords: coronavirus; COVID-19; drug designing; gamma-glutamyl-S-allylcysteine; herbal drug; hydroxychloroquine; molecular docking

Introduction

Coronaviruses (CoVs) represent a category of infectious agents, belonging to the family Coronaviridae, categorized into four genera, namely, alpha-CoV, beta-CoV, gamma-CoV, and delta-CoV along with their subclasses [1]. The novel COVID-19 pandemic is associated with the SARS-CoV-2 virus which belongs to the beta-CoV genera and originated from the Hubei province of Central China during late November 2019, with its epicenter being in Wuhan city harboring nearly 11 million people [1, 2]. This infection has been growing since then and has spread to more than 218 countries [3, 4]. The transmissibility and penetrance rate of this infection is frequently changing on an hourly and daily basis [5, 6]. The incubation period of SARS-CoV-2 ranges between 1–14 days with the median incubation period of about 5 days. An infected person may show symptoms after the median incubation period. However, the infected individual can spread the infection by contracting the disease without showing overt symptoms. The primary mode of transmission of SARS-CoV-2 infection is through contact with the infected individuals and/or by respiratory droplets [7]. Some studies have also proposed that SARS-CoV-2-infected or cured individuals can transmit the virus via fecal shedding [8].

The exact molecular pathogenesis of SARS-CoV-2 is yet not known with certainty; however, it has been proposed that viral pathogenesis is triggered by the release of proinflammatory cytokines that are associated with the activation of several signaling pathways, namely, TLRs-dependent IFN induction pathways (interferon regulatory transcription factor, *i.e.*, IRF-3/7 & nuclear factor kappa-light-chain-enhancer of activated B cells, *i.e.*, NF-Kβ) and myeloid differentiation primary response 88 (MyD88) pathways (*e.g.*, Activating transcription factor, *i.e.*, ATF-2 & Activator protein, *i.e.*, AP-1). The primary virulence factors of the virus include SARS-CoV-2 spike glycoprotein (viral envelope protein responsible for viral attachment and entry into the host cells); viral nuclease (NSP15 endoribonuclease responsible for mediating viral capsid formation); and protease (Main Protease 3CLpro responsible for viral capsid formation) [9]. SARS-CoV-2 mainly targets the alveolar and bronchial epithelial cells. The viral spike glycoprotein interacts with the ACE-2 receptors of the host cell, thereby mediating the viral entry [10]. Afterward, there occurs an elevated release of proinflammatory cytokines (IL-6 and IL-12), chemokines (IL-8, CCL-2, and CXCL10), and interferon. The virus gets hold of the host cell machinery and manipulates it for driving the process of viral replication. The virus also attempts to inhibit the production of interferon and proinflammatory cytokines employing RNA helicases and non-structural proteins (NSP 1, 3, 7 & 15). Subsequently, the viral load keeps on rising within the host system, ultimately leading to viremia (**Fig. 1**).

Meanwhile, the host immune system also strives to fight back. The further spread of the virus within the host system depends on the immunological status of the host. Immunomodulatory remedies play a pivotal role at this phase, wherein such moieties may mediate the transformation of an immunocompromised individual to an immunocompetent one. The structure and sequence of SARS-CoV-2 have been identified and drug screening followed by clinical trials are continuously being conducted by targeting these virulence factors [10]. However, there are no approved drugs for effectively managing COVID-19 infection, probably due to unidentified dynamic pathophysiology; high mutagenicity of the virus; and adverse side effects of earlier known Coronavirus vaccines and drugs [11, 12]. Herbals provide a unique solution in terms of their negligible side effects, synergistic activity, broad-spectrum therapeutic ability, and immunomodulation effects. Several studies have been conducted to screen phytocompounds as novel drug candidates for mitigating the Corona virus. Various phytocompounds have been found to show significant inhibition against various target viral proteins of SARS-CoV-2 as depicted from molecular docking studies performed at an *in-silico* level. Recently, amentoflavone and gallocatechin gallate have been suggested as propitious inhibitors of 3CLpro and PLpro proteins of SARS-CoV-2 [13]. Similarly,

asparosides found in *Asparagus racemosus* also depicted significant docking score and affinity against NSP15 Endoribonuclease and spike receptor-binding domains of SARS-CoV-2 [14].

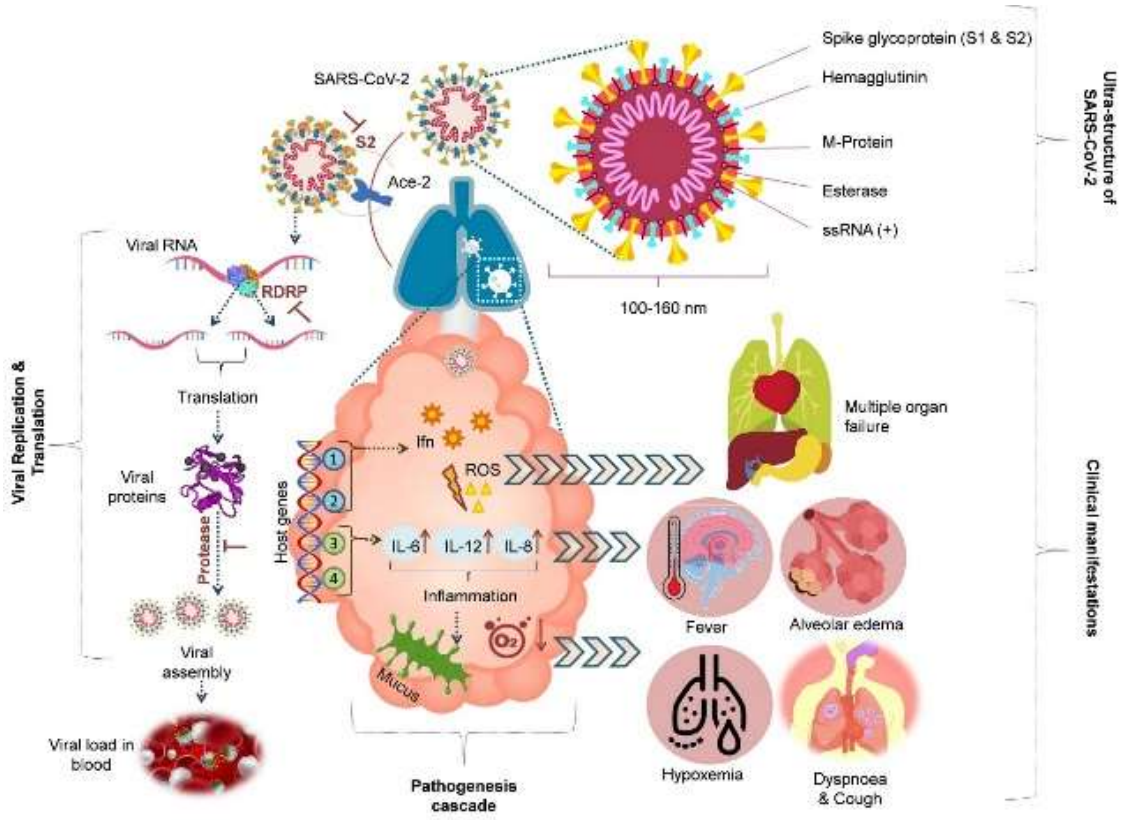

Figure 1. Molecular Pathogenesis & Clinical manifestations of Novel Coronavirus (SARS-CoV-2).
SARS-CoV-2 infects lung parenchymal cells and upon entering the host bronchial cells, the virus elicits an immunological response. Subsequently, inflammatory cytokines, interferon-gamma, and reactive oxygen species are produced. SARS-CoV-2 gets hold of host metabolic machinery and initiates its replication and translation

Similarly, a multitude of medicinal plants containing various phytochemicals have been found to show similar *in silico* docking score, against one or the other target proteins of SARS-CoV-2 [15, 16]. However, many phytoconstituents that exhibit significant docking scores often violate the Lipinski score-based drug likeliness (high molecular mass, extremely high reactivity, and low bioavailability) and hence could not be used for further therapeutic usage. Furthermore, various phytomolecules screened via the *in-silico* docking analysis may exhibit high toxicity and mutagenicity. Hence, toxicity/mutagenicity descriptors should also be analyzed while finalizing the phytomolecules for further *in vitro* or *in vivo* analysis.

In the present study, the drug-like potential of secondary metabolites of herbal origin will be studied by targeting SARS-CoV-2 spike glycoprotein (S2), viral nuclease (NSP15 endoribonuclease), and protease (Main Protease 3CLpro). The selection of herbal secondary metabolites is based on investigating the potency of various herbals showing resistance towards viral virulence factors as indicated by various scientific search engines based on priority indexing. All the selected herbal moieties were subjected to molecular docking using Hex software, to assess the interactions of phytoligands with the target viral proteins. Further screening of the propitious herbal leads was conducted by assessing the *in-silico* toxicity and Lipinski score-based drug likeliness (*i.e.*, a molecule with molecular mass less than 500 Da, no more than 5 hydrogen bond donors, no more than 10 hydrogen bond acceptors, and an octanol-water partition coefficient log P not greater

than 5). Bulk outliers showing high toxicity/mutagenicity or violating the Lipinski rules were eliminated. Subsequently, the drug-receptor interaction of the filtered herbal moieties was studied to obtain a lead molecule that could be further tested at preclinical and clinical levels. Although the search for potential leads targeting the novel Coronavirus will continue perpetually, these herbal leads may serve to be highly beneficial owing to their antiviral activities, potentiating nature, and symptomatic relief provision capabilities, presented along with limited toxicities and comprehensive treatment strategy.

2. Materials and Methods

2.1 Preparation of viral virulence factors as receptors

The crystal structures of relevant protein targets, namely, SARS-CoV-2 spike glycoprotein (S2; PDB code: 6VSB, Pre-fusion conformation), viral nuclease (NSP15 endoribonuclease; PDB code: 6VWW), and protease (Main Protease 3CLpro; PDB code: 1Q2W) were obtained from RCSB Protein Data Bank (https://www.rcsb.org/). These structures were examined critically using Ramachandran Plot by ProCheck to validate the modeled protein structures based on the ϕ (phi), ψ (psi), and ω (omega) angles, thereby inspecting the quality of the target protein structures selected for docking studies. Furthermore, hydrogen atoms were introduced in all these 3D structures using Argus Lab (4.0.1), to customize the target viral proteins for rigid docking (http://www.arguslab.com/arguslab.com/ArgusLab.html).

2.2 Active site analysis of viral virulence factors

The prediction of active sites of target viral proteins was accomplished by DoG Site Scorer, and the Cartesian coordinates x, y, z (active sites) for effective docking were visualized in Argus Lab. These regions were further used for the generation of grid boxes for docking studies by Hex Cuda 8.0.0.

2.3 Selection and preparation of herbals as promising anti-SARS-CoV-2 candidates

A total of 24 bioactive compounds from naturally available medicinal plants were selected by employing a biostatistical matrix-based analysis. Based on the understanding of the pathophysiological targets of the novel Coronavirus, herbal candidates exhibiting inhibitory properties specific to the viral virulence factors were searched in the PubMed repository. The descriptors used for conducting a PubMed search with the help of an extensive literature search included keywords as 'virulence factor inhibition + herbal moiety'. The binary coefficient for the said herbal moieties was calculated by assessing the presence or absence of particular inhibiting properties exhibited against the individual physiological target. The presence of an inhibiting property in a said herbal moiety was marked as 1, otherwise, a score of 0 was assumed. The cumulative binary score for each plant ranged between 0 to 6, wherein the median cut-off value was selected as 3. Plants having a binary score ≥ of 3 were considered for further weightage-based matrix analysis, wherein the binary score of each plant was multiplied with the relevance score of the viral virulence factor. Ultimately, a fuzzy set membership analysis was conducted to obtain a universal score for each plant. The fuzzy set score ranged between 0 and 1, wherein the plants with a fuzzy score greater than 0.5 were further selected for assessing their specific anti-SARS-CoV-2 activity.

$$\mu S = (S-\min S)/(\max S-\min S), \quad (1)$$

where, μS represents the desirability values of members of the fuzzy set S; min(S) and max(S) are minimum and maximum values, respectively, in the fuzzy set S [17].

The three-dimensional structures of all these bioactive molecules as well as the reference drug compound, *i.e*., hydroxychloroquine was retrieved from the PubChem database. The ligand molecules were then converted into PDB format using Open Babel (2.4) interface (openbabel.org/docs/dev/OpenBabel.pdf), as required for rigid docking.

2.4 In silico pharmacokinetic analysis - Drug Likeliness

Drug likeliness of the selected phytoligands (~ 17 compounds) was assessed by using Drug likeness tool Dru Li to which is an open-source virtual screening tool for calculating Lipinski's

rule of five, *i.e*., molecular weight, number of hydrogen bond donors, number of hydrogen bond acceptors and LogP value (http://www.niper.gov.in/pi_dev_tools/DruLiToWeb/DruLiTo_index.html). Violation of more than one rule would cause exclusion of the said phytochemical. The rest of the selected phytoligands were subjected to ADMETox analysis [17].

2.5 In silico pharmacokinetic analysis - ADMETox Analysis

The ADMETox (Absorption, Distribution, Metabolism, Excretion, and Toxicity) descriptors of the selected phytocompounds were predicted by conducting admetSAR. The estimation of the probability values of the compounds for diverse profiles including human oral bioavailability, human epithelial colorectal adenocarcinoma cell (CaCo2) permeability, logP for substrates and inhibitors, predicted aqueous solubility, and different toxicity profiles in terms of Ames toxicity and oral toxicity (LC_{50} and LD_{50} values) were computationally predicted. Phytomolecules exhibiting toxic profiles as assessed in the *in-silico* toxicity analyses were excluded from the study. The rest of the selected phytoligands were subjected to molecular docking analysis.

2.6 Molecular Docking and Ligand Receptor Binding analysis

The docking analysis of PDB structures of selected phytoligands (excluding the Lipinski rule and ADMETox violating moieties) with target viral proteins (spike glycoprotein, viral nuclease, and viral main protease) was carried by Hex Cuda 8.0.0 software. Receptor and Ligand files were imported into the software. The grid dimension of docking was defined according to the binding site analysis of DoG Site Scorer. Graphic settings and Docking parameters were customized to calculate the binding energies (E values) of ligand-receptor docking. All Hex based docking correlations mentioned in this manuscript used fast Fourier transform (FFT) correlation techniques for estimating the rigid ligand-receptor interaction. Various orientations of ligand and receptor docking were assessed within the system assembly itself (N= 25,000 orientations). All the orientations were re-scored according to the shape and electrostatic correlations as well, to deduce a final binding energy score for each interaction. The free binding energy of the receptor-ligand complex was calculated by summating the number of free rotatable bonds and contact energy. The underlying mathematical equation used for deducing the free binding energy has been given below.

$$\Delta \mathbf{G} = \mathbf{Gcomplex} - [\mathbf{G\ receptor} + \mathbf{G\ ligand}] \quad (2)$$

The best-docked conformations with the lowest docking energy were selected for further MD simulations using Pose View for creating pose depictions of selected ligand-receptor binding [18].

3. Results

3.1 Quality assessment of viral virulence factors

The first quality assessment of the selected viral virulence factors (SARS-CoV-2 spike glycoprotein S2, viral NSP15 endoribonuclease, and main protease 3CLpro) was carried out using Ramachandran plot analysis computed with ProCheck. The analysis showed that residues of SARS-CoV-2 spike glycoprotein S2, viral NSP15 endoribonuclease, and main protease 3CLpro in the most favorable region were 84%, 93.1%, and 89.6%, respectively. Moreover, in the additionally allowed regions, nearly 15.9%, 6.9%, and 9.6% residues of SARS-CoV-2 spike glycoprotein S2, viral NSP15 endoribonuclease, and main protease 3CLpro were found, respectively.

The detailed secondary structural investigation of the SARS-CoV-2 spike glycoprotein S2 with PDB sum server revealed that 313 (10.77%) residues were in strands, 2112 (72.70%) residues were in α-helices, 78 (2.68%) residues were in β-turns and 402 (13.83%) residues were in other conformations. Similarly, the PDB sum secondary structure of NSP15 endoribonuclease revealed that 72 (10.34%) residues were in strands, 577 (82.90%) residues were in α-helices, 4 (0.57%) residues were in β-turns and 43 (6.17%) residues were in other conformations. Moreover, PDB sum secondary structure of main protease 3CLpro revealed that 75 (12.66%) residues were in strands, 457 (77.19%) residues were in α-helices, 7 (1.18%) residues were in β-turns and 53 (8.95%) residues were in other conformations (**Fig. 2**).

The presence of these residues within permissible limits suggests that all the selected receptors are stereo-chemically fit for molecular docking analysis. Prevalence of α-helices, *i.e.*, more than 70%, ensures conformational stability and robustness to all the three viral virulence factors. Moreover, a minor presence of β-turns (~less than 3%) also allows the polypeptide chains of the viral virulence factors to reverse their direction at appropriate configurational foci, thereby exposing the respective active site of binding for proper orientation and docking of the target viral proteins with the phytoligands.

3.2 Active site analysis of target viral proteins

Active site analysis of SARS-CoV-2 spike glycoprotein (S2), viral nuclease (NSP15 endoribonuclease) and protease (Main Protease 3CLpro) as conducted by DoG Site Scorer indicated that there are various active pockets within the studied viral virulence factors with druggability ranging from 0.12 to 0.86 (**Table 1**). It was found that pockets P_11 (Drug score: 0.847), P_1 (Drug score: 0.860), and P_0 (Drug score: 0.805) were energetically favorable for performing further molecular docking studies with the target viral proteins being spike glycoprotein, NSP15 endoribonuclease, and Main Protease 3CLpro, respectively.

3.3 Selection of herbals as promising anti-SARS-CoV-2 candidates

Extensive literature surge combined with a matrix-based analysis was conducted for the selection of plants having probable utility against SARS-CoV-2. The parameters for selecting the herbals included - a) ethnopharmacological importance of the plant; b) prior pharmaco-therapeutic investigations of the plant; and c) symptomatic relief providing capabilities of the plant. Binary, weightage, and fuzzy score analyses were conducted for all the plants to screen for herbals exhibiting probable anti-SARS-CoV-2 activity. Plants showing positive assessment for more than 03 parameters, reported in PubMed search engine were selected for further *in silico* analysis. The rationale for selected plants (~18 phytomolecules) along with their binary, weightage, and fuzzy scores has been explained in **Table 2**.

3.4 Pharmacokinetic descriptors of phytoligands

Drug likeliness characteristics of the bioactive phytoligands were assessed by employing a step-wise filtering strategy, wherein various physiochemical properties such as log P, H-bond acceptor, H-bond donor, molecular weight, acidic groups, aromatic rings, number of rotatable bonds and chains, number of hydrogen bonds and molar refractivities were predicted to evaluate the drug-like behavior of the phytoligand. The Lipinski scores for the selected phytomolecules were found to be within acceptable ranges as elucidated in **Table 3**. However, one of the herbal moieties, namely, Gallotannin was eliminated at this stage as it violated more than 2 'Lipinski rules' of drug likeliness.

3.5 ADMETox prediction of phytoligands

ADMETox prediction of the phytoligands was done by using admetSAR tool which is a freely available comprehensive source for prediction of ADMET (Absorption, distribution, metabolism, excretion, and toxicity) properties. admetSAR is an open-source tool with a database of more than 96,000 compounds, wherein the ADME values (Absorption, distribution, metabolism, excretion), mutagenicity, and toxicity profile can be easily searched. *In silico* prediction of ADMETox as mediated by admetSAR tool will aid in assessing the safety of the phytomolecules to be developed as drug candidates in the coming future. The results of admetSAR prediction showing the probability values are summarized in **Table 4**. The phytoligands violating any of the ADMETox descriptors (amentoflavone, butenolide, malic acid, β-myrcene, paeoniflorin) were excluded at this step itself. The rest of the phytoligands (~ 12 moieties) did not exhibit any mutagenic or toxic profile. Based on the predicted probability values, the selected phytoligands were known to get absorbed efficiently by the intestinal epithelium as the values for CaCo2 permeability and intestinal absorption were found to be within permissible range (~ absorption value ≥ 0.5). The aqueous solubility of the selected phytoligands was also predicted to be acceptable (logS ≥ - 4). Most of the selected phytoligands also exhibited efficient binding with the plasma protein and did not exhibit any

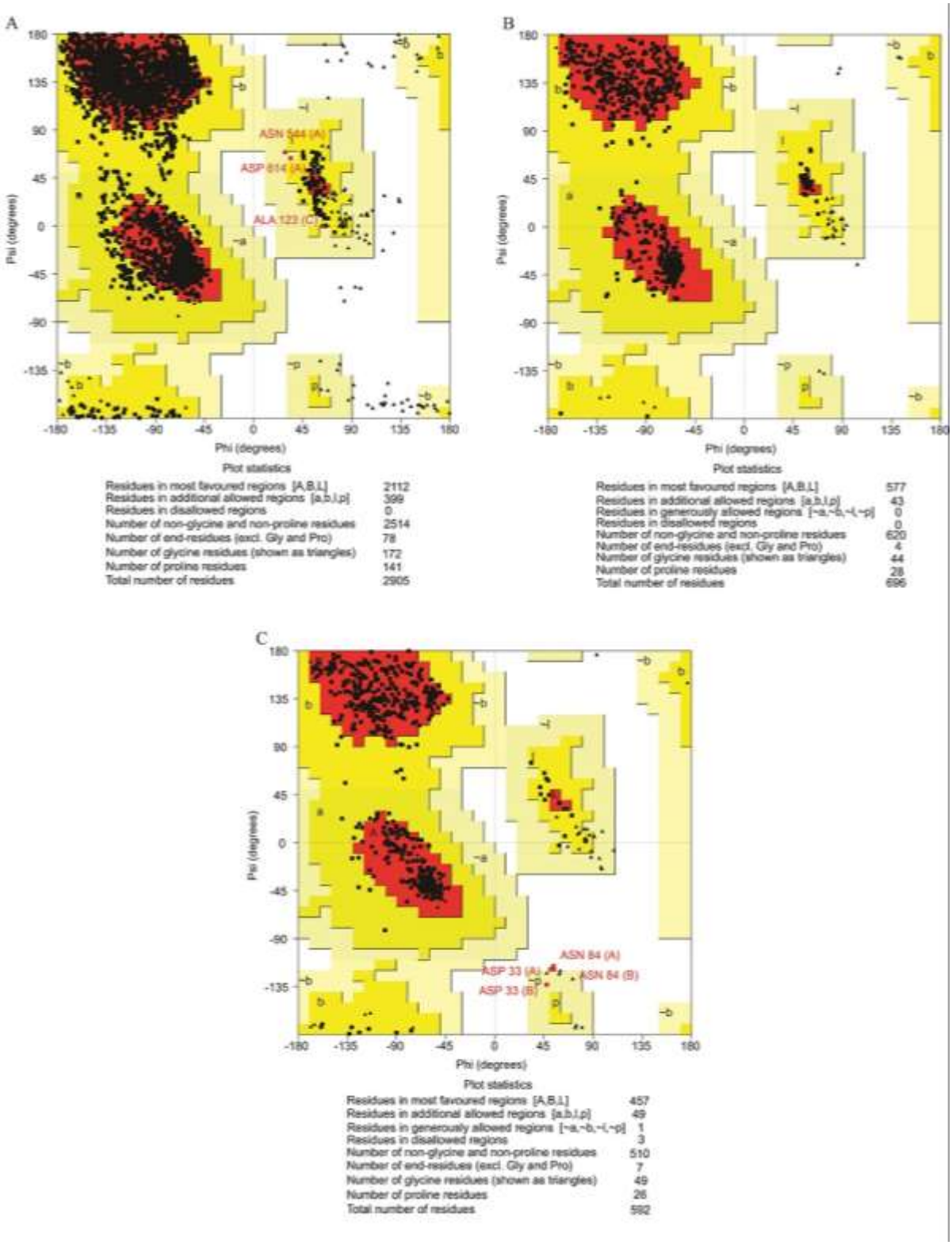

Fig. 2. Ramachandran plot of the structure models of SARS-CoV-2 target proteins - (A) Spike glycoprotein, (B) NSP15 endoribonuclease, and (C) Main protease 3CLpro.

The most favored regions are colored in red and marked as A, B, and L. The additionally allowed regions are colored in yellow and marked as a, b, l, and p. All non-glycine and proline residues are shown as filled black squares, whereas glycine residues (non-end) are shown as filled black triangles. Disallowed residues are represented by white color. Abbreviations: Asn: asparagine; Asp: aspartate; Gly: glycine; Pro: proline.

Table 1. Active pockets and corresponding pocket area, volume, enclosure, and druggability indices for SARS-CoV-2 virulence factors.

Viral Virulence Factor (PDB ID)	Total Pockets	Active pockets†	Area (Å^2)	Volume (Å^3)	Enclosure (Å)	Hydrophobicity (Kcal/ Å^2)	Drug Score	Representation
Spike glycoprotein (6VSB)	106	P_11	807.13	662.19	0.06	0.27	0.84	
		P_7	1027.4	885.73	0.16	0.31	0.83	
		P_9	792.72	781.17	0.08	0.24	0.82	
		P_10	987.15	728.29	0.08	0.44	0.82	
		P_6	1194.9	1024.5	0.17	0.42	0.81	
NSP15 endoribonuclease (6VWW)	31	P_1	787.38	683.48	0.06	0.24	0.86	
		P_0	712.51	685.95	0.08	0.25	0.85	
		P_3	561.74	467.99	0.23	0.46	0.78	
		P_2	832.74	507.64	0.14	0.54	0.76	
		P_5	621.35	344.13	0.07	0.45	0.70	
Main Protease 3CLpro (1Q2W)	11	P_0	2867.9	2443.7	0.12	0.33	0.80	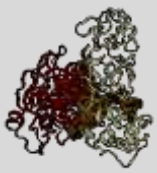
		P_1	589.09	364.2	0.2	0.59	0.75	
		P_2	341.62	297.14	0.25	0.48	0.47	
		P_4	430.51	222.15	0.25	0.44	0.47	
		P_3	373.5	237.35	0.25	0.25	0.46	

†Only the most active pockets have been presented with a high druggability score; Shaded rows indicate the most druggable pockets which will be further employed for docking studies.

inhibition of CYP3A4 or P-glycoprotein or any other toxicities.

3.6 Molecular Docking analysis

Docking results of the viral virulence factors, namely, spike glycoprotein, NSP15 endoribonuclease, and Main Protease 3CLpro; and the selected phytoligands (~ 12 phytomolecules) are shown in **Table 5**. These docking-based E values have also been compared with that of the standard drug, *i.e*., hydroxychloroquine. Hex based docking results revealed that the E-value of docking of gamma-glutamyl-S-allylcysteine and salvianolic acid with all the selected target viral proteins (viral main protease 3CLpro, spike glycoprotein, and NSP15 endoribonuclease) was significantly better as compared to hydroxychloroquine. Several other phytoligands also showed comparable binding energies concerning at least one of the target viral proteins; however, none of the other phyto-moieties exhibited holistic docking abilities. Hence, it is obvious from the E-values that gamma-glutamyl-S-allylcysteine and salvianolic acid bind spontaneously and irreversibly to all the tested viral proteins, thereby these phytomolecules might be having the potential to block the spread and replication of the SARS-CoV-2 virus. Moreover, the binding efficiency of gamma-glutamyl-S-acetylcysteine is exceedingly better than that of salvianolic acid. However, all these *in silico* findings need to be substantiated with clinical studies.

3.7 Phytoligand and viral proteins binding pose depictions.

The best-docked conformations with the lowest docking energy, *i.e*., gamma-glutamyl-S-allylcysteine and salvianolic acid were selected for further MD simulations using Pose View for creating pose depictions of selected ligand-receptor binding. Upon assessing the binding pose and electrostatic bridging interactions, it was found that only gamma-glutamyl-S-allylcysteine (Herbal source: *Allium sativum*) was able to fit into the active binding pockets of the

Table 2. Selected Herbal moieties showing probable antiviral utility as assessed by employing extensive literature surge.

Plant Source§	**Predominant phytocompound**	***Search-engine based literature surge***			***In silico Bioprospection based analysis***			***From previous studies***	**Ref**
		Activity explored†			**Binary Score**	**Weightage Score**	**Fuzzy Score***	**Probable antiviral utility**	
		S2	NSP 15	3CL pro					
Alisma canaliculatum A. Braun & C.D.Bouché	Alisol A 24-Acetate	+	–	–	2	1.16	0.46	Anti-influenza activity is observed as the herbal moiety inactivates the hemagglutinin spike receptor.	[19]
Allium cepa L.	Allicin	+	+	+	3	1.66	0.66	Hinders virus attachment to host cell, alter transcription and translation of viral genome in a host cell and also affect viral assembly.	[20]
Allium sativum L.	Gamma-Glutamyl-S-allylcysteine	+	+	+	6	2.49	1	Acts as protease inhibitor mainly.	[20]
Asparagus racemosus Willd.	Isoasparagine	–	–	–	3	0.40	0.3	Symptomatic alleviation in case of herpes virus infection.	[21]
Berberis aristata DC.	Berberine	+	–	+	5	1.91	0.76	Inhibits enterovirus 71 entry and replication by downregulating the MEK/ERK signaling pathway and autophagy.	[22]
Boswellia serrata Roxb.	11-keto-beta-boswellic acid	+	–	+	3	1.66	0.66	Inhibits Chikungunya and Vesicular stomatitis virus infections by blocking their entry.	[23]

Plant Source§	**Predominant phytocompound**	***Search-engine based literature surge***			***In silico Bioprospection based analysis***			***From previous studies***	**Ref**
		Activity explored†			**Binary Score**	**Weightage Score**	**Fuzzy Score***	**Probable antiviral utility**	
		S2	NSP 15	3CL pro					
Camellia sinensis (L.) Kuntze	Quercetin	+	−	+	5	1.91	0.76	Suppressed Hepatitis C virus entry, and also inhibited viral RNA replication.	[24]
Chlorophytum borivilianum Santapau & R.R. Fern.	Neotigogenin	−	−	−	2	0.40	0.3	Cytokine modulating potential.	[25]
Curcuma longa L.	Curcumin	+	−	+	5	1.91	0.76	Inhibits entry of Chikungunya and Vesicular stomatitis virus.	[23]
Epimedium flavum Stearn	Wushanicariin	+	−	−	1	1	0.4	Induced the secretion of type I IFN and pro-inflammatory cytokines.	[26]
Gingko biloba L.	Amentoflavone	+	−	+	4	1.66	0.66	Inhibits viral protease, specifically in case of HIV infection.	[27]
Houttuynia cordata Thunb.	β-myrcene	+	−	+	5	1.91	0.76	Inactivation of 3C-like proteinase of murine Coronavirus and dengue virus.	[28]
Melissa officinalis L.	Citronellal	+	+	−	5	1.49	0.59	Inhibition of HIV-1 protease.	[29]
Ocimum tenuiflorum L.	Carvacrol	−	−	+	3	0.75	0.35	Inactivation of viral protease in case of HIV infection.	[30]
Paeonia lactiflora Pall.	Paeoniflorin	+	−	−	3	1.41	0.56	Inhibits viral entry in case of Influenza virus infection.	[31]

Plant Source§	Predominant phytocompound	*Search-engine based literature surge*			*In silico Bioprospection based analysis*			*From previous studies*	Ref
		Activity explored†			**Binary Score**	**Weightage Score**	**Fuzzy Score***	**Probable antiviral utility**	
		S2	NSP 15	3CL pro					
Phyllanthus amarus Schumach. & Thonn.	Gallotannin	−	+	+	5	1.49	0.59	Halts the process of viral replication in case of Herpes simplex virus infection.	[32]
Rheum rhabarbarum L.	Malic acid	+	−	+	4	1.91	0.76	Inhibits viral entry by ceasing the endosomal fusion in case of influenza virus.	[33]
Salvia miltiorrhiza Bunge	Salvianolic acid	−	+	+	5	1.49	0.59	Inhibition of HIV-1 integrase and protease.	[34]
Taxillus sutchuenensis var. *duclo uxii* (Lecomte) H.S.Kiu	Butenolide	+	−	+	2	1.5	0.60	Inhibition of Hepatitis C viral NS3 serine protease and ceasing viral entry.	[35]
Tinospora cordifolia (Willd.) Hook.f. & Thomson	Tinosporaside	+	+	+	5	2.49	1	Immunomodulatory activity: Anti-HIV activity wherein it acts as viral ribonuclease inhibitor.	[36]
Withania somnifera (L.) Dunal	Withanolide	+	+	+	3	1.41	0.56	Disrupts interactions between viral S-protein receptor binding domain and Host ACE2 receptor.	[37]
Zingiber officinale Roscoe	6-Gingerol	−	+	+	5	1.49	0.59	Inhibits Hepatitis C virus protease.	[38]

§Plants are selected based on extensive literature surge, specifically focusing on their ethnomedicinal attributes, symptomatic relief provision abilities, and direct/indirect antiviral activity, if any.

†Symbols of + and – denote the presence and absence of viral virulence factor inhibitory properties in the given plant, as deduced based on keyword search matrix analysis using the PubMed search engine.

**Fuzzy score μS = (S-minS)/ (maxS-minS), wherein shaded cells represent the ligands selected for further study with a fuzzy score > 0.5.*

Table 3. Physicochemical properties of phytoligands in comparison with the standard chemotherapeutic agent.

Ligand/ Standard	Physicochemical Properties				
	Mol. Wt. (≤ 500 D)[A]	**Log P (≤ 5)†[B]**	**H-Bond Donor (≤ 5)[C]**	**H-Donor Acceptor (≤ 10)[D]**	**Lipinski violations (if any)***
Allicin	162.02	0.237	0	1	0
Amentoflavone	538.09	2.030	6	10	1[A]
Berberine	336.12	2.473	0	4	0
Beta-caryophyllene	204.19	6.044	0	0	1[B]
11-keto-beta-boswellic acid	470.34	8.131	2	4	1[B]
Butenolide	84.02	0.308	0	2	0
Citronellal	154.14	3.591	0	1	0
Curcumin	368.13	1.945	2	6	0
Gallotannin	1700	9.537	25	46	4[A, B, C, D]
Gamma-Glutamyl-S-allylcysteine	290.09	-2.68	4	7	0
6-Gingerol	294.18	2.437	2	4	0
Malic acid	134.02	-1.474	3	5	0
β-myrcene	136.13	4.170	0	0	0
Paeoniflorin	480.16	-0.464	5	11	1[D]
Quercetin	302.04	1.834	5	7	0
Salvianolic acid	494.12	2.898	7	10	1[C]
Tinosporaside	492.20	0.54	4	10	0
Withanolide	470.27	3.263	2	6	0
Hydroxychloroquine	335.88	4.00	4	2	0

†Logarithm of compound partition coefficient between *n*-octanol and water.

*Shaded cell indicates phytoligand with more than 1 Lipinski violations and hence is eliminated at this stage itself.

Note: Parameter of Lipinski violation has been superscripted in the form of alphabets to indicate the specific physicochemical property that is beyond permissible limits.

Table 4. ADMETox values of phytoligands in comparison with the standard chemotherapeutic agent.

Ligand/ Standard	Absorption		Distribution		Metabolism		Excretion	Toxicity
	Caco-2 permeability (value ≥ 0.5)	Human intestinal absorption (value ≥ 0.5)	Plasma Protein binding (value ≥ 0.5)	Water solubility (logS ≥ - 4)	P-glyco-protein activator (value ≥ 0.5)	CYP3A4 inhibition (value ≥ 0.5)	Acute oral toxicity (Kg/mol) (value ≥ 1.0)	Ames test (value ≥ 0.5)
Allicin	0.58 (+)	0.91 (+)	0.50 (+)	-0.89 (+)	0.98 (+)	0.92 (-)	1.935 (-)	0.61 (-)
Amentoflavone	0.87 (+)	0.98 (+)	1.11 (+)	-3.36 (+)	0.44 (-)	0.61 (-)	1.822 (-)	0.68 (-)
Berberine	0.94 (+)	0.77 (+)	0.83 (+)	-2.97 (+)	0.68 (+)	0.58 (-)	1.545 (-)	0.75 (-)
Beta-caryophyllene	0.86 (+)	0.98 (+)	0.83 (+)	-4.68 (+)	0.89 (+)	0.86 (-)	2.366 (-)	0.99 (-)
11-keto-beta-boswellic acid	0.54 (+)	0.99 (+)	1.05 (+)	-3.45 (+)	0.63 (+)	0.79 (-)	2.834 (-)	0.82 (-)
Butenolide	0.76 (+)	0.96 (+)	0.096 (-)	0.23 (+)	0.98 (+)	0.98 (-)	1.976 (-)	0.77 (-)
Citronellal	0.92 (+)	0.97 (+)	0.70 (+)	-2.44 (+)	0.98 (+)	0.96 (-)	2.307 (-)	0.99 (-)
Curcumin	0.76 (+)	0.97 (+)	0.83 (+)	-3.36 (+)	0.59 (+)	0.53 (-)	1.992 (-)	0.96 (-)
Gamma-Glutamyl-S-allylcysteine	0.92 (+)	0.63 (+)	0.50 (+)	-1.68 (+)	0.93 (+)	0.74 (-)	1.648 (-)	0.55 (-)
6-Gingerol	0.59 (+)	0.99 (+)	0.85 (+)	-3.23 (+)	0.89 (+)	0.59 (-)	2.290 (-)	0.57 (-)
Malic acid	0.95 (+)	0.77 (+)	0.23 (-)	0.27 (+)	0.98 (+)	0.90 (-)	0.844 (+)	0.87 (-)
β-myrcene	0.77 (+)	0.96 (+)	0.43 (-)	-3.44 (+)	0.98 (+)	0.66 (-)	1.660 (-)	0.92 (-)
Paeoniflorin	0.82 (+)	0.41 (-)	0.67 (+)	-2.97 (+)	0.65 (+)	0.85 (-)	3.502 (-)	0.53 (-)
Quercetin	0.64 (+)	0.98 (+)	1.17 (+)	-2.99 (+)	0.91 (+)	0.69 (-)	2.559 (-)	0.90 (-)
Salvianolic acid	0.93 (+)	0.96 (+)	1.03 (+)	-3.20 (+)	0.65 (+)	0.83 (-)	2.069 (-)	0.58 (-)
Tinosporaside	0.84 (+)	0.83 (+)	0.50 (+)	-3.65 (+)	0.54 (+)	0.75 (-)	3.236 (-)	0.70 (-)
Withanolide	0.62 (+)	0.97 (+)	1.18 (+)	-4.00 (+)	0.51 (+)	0.85 (-)	3.660 (-)	0.78 (-)
Hydroxy-chloroquine	0.66 (+)	0.99 (+)	0.86 (+)	-4.00 (+)	0.84 (+)	0.83 (-)	2.684 (-)	0.70 (-)

**Denoted '+' or '-' sign relates to the presence or absence of a predicted activity, respectively. Shaded cells indicate the descriptors violating the standard values, thereby excluding the respective phytoligand(s) from further studies.*

Table 5. Molecular Docking of selected phytoligands and standard chemotherapeutic agent with SARS-CoV-2 viral virulence factors.

Ligand / Standard	E Value (Kcal/mol)[§]		
	Main Protease 3CLpro	Spike glycoprotein	NSP15 endoribonuclease
Allicin	-121.34	-108.38	-157.34
Berberine	-211.64	-179.51	-240.83
Beta-caryophyllene	-129.23	-132.62	-176.22
11-keto-beta-boswellic acid	-253.66	-199.35	-269.92
Citronellal	-139.41	-134.74	-160.92
Curcumin	-213.59	-197.87	-247.25
Gamma-Glutamyl-S-allylcysteine	-493.53	-578.57	-825.00
6-Gingerol	-199.85	-178.86	-221.35
Quercetin	-189.57	-158.27	-204.25
Salvianolic acid	-261.56	-223.97	-275.44
Tinosporaside	-233.14	-223.92	-268.79
Withanolide	-207.18	-214.98	-253.37
Hydroxy chloroquine	-235.48	-207.47	-213.54

[§]$\Delta G_{binding} = \Delta G_{complex} - (\Delta G_{receptor} + \Delta G_{ligand})$; Grey shaded cells indicate highly significant E value of docking as compared to the standard chemotherapeutic agent; Green shaded cells indicate holistic phytoligands exhibiting optimum E value for all the three selected viral virulence factors (These phytoligands have been further analyzed for salt-bridge analysis and electrostatic interactions).

target viral proteins, whereas salvianolic acid could not establish an irreversible and spontaneous bond with the target viral proteins. The orientational binding of gamma-glutamyl-S-allylcysteine and the target viral proteins showing the pose view and residue interactions have been depicted in **Fig. 3**. It was observed that the amide group of gamma-glutamyl-S-allylcysteine formed a hydrogen bond with the amide residue of glutamine amino acid (1071st position) found in the viral spike glycoprotein. Chemical bridging of gamma-glutamyl-S-allylcysteine and glutamic acid residues of viral endoribonuclease present a similar case where glutamic acid residues (45th position) were invariably bound and neutralized, thereby possibly neutralizing the COVID-19 virus. Similarly, the hydroxyl group of gamma-glutamyl-S-allylcysteine formed a hydrogen bond with the carbonyl group of proline amino acid (108th position) of viral main protease.

4. Discussion

The spike glycoprotein of SARS-CoV-2 is required for initiating the attachment and entry of the virus into the host cell. Moreover, viral main protease 3CLpro is fundamental for continuing the viral life cycle of SARS-CoV-2 as it is required by the virus to catalyze the cleavage of viral polyprotein precursors which are ultimately necessary for viral capsid formation and enzyme production [39]. Similarly, NSP15 endonucleases are necessary for catalyzing the processing of viral RNAs and hence are required for enduring the process of viral replication [5]. These target viral proteins were selected as drug targets for mitigating the novel coronavirus. Thereafter the stereo-chemical applicability of the target viral proteins (spike glycoprotein, main protease, and endonuclease) was analyzed by using Ramachandran plot as computed with ProCheck and PDB Sum. It was observed that all of the target viral proteins exhibited favorable stereo-chemical parameters and hence, the 3D

structures of all these receptors correspond to high-probability conformation for molecular docking [40]. Furthermore, the active site of these receptors was analyzed by using the DoG Site Scorer. While conducting the active site analysis, the DoG Site Scorer tool analyzed the heavy atom coordinates on the surface of the 3D structure of the respective target viral proteins. Depending on these atomic coordinates, a hypothetical grid was spanned by out ruling the chances of any spatial overlap of the grid with the heavy atoms. Furthermore, the tool engages in applying a Gaussian filter to the defined grids, to identify spherical pockets of binding. Druggability score (0-1) of the selected spherical pockets are deduced based on their surface area, volume, enclosure, and hydrophobicity. As a general rule, a higher druggability score is indicative of a more druggable pocket [41].
After optimizing the most virulent drug targets (target viral proteins), the prospective selection of herbal drug moieties was performed by using PubMed based keyword hits matrix analysis. The drug likeliness and ADMETox descriptors of the selected herbal ligands were computationally predicted. According to Lipinski's rule, a drug like a moiety should have low molecular weight (≤ 500 D), log P value ≤ 5, number of hydrogen bond acceptors ≤10, and number of hydrogen bond donors ≤5. A bioactive druggable molecule should ensue to at least 4 of the 5 Lipinski rules [42]. Nearly 12 out of 24 tested phytomolecules were found to druggable following the drug likeliness and ADMETox descriptors.

All the selected phytoligands (as depicted in **Table 4**) were known to get absorbed efficiently by the intestinal epithelium (CaCo2 permeability and intestinal absorption value ≥ 0.5). Hence, these phytoligands may get easily transported after getting absorbed in the human body. They also exhibited efficient binding with the plasma protein, thereby ensuring efficient distribution of the probable drug moieties (Plasma protein binding value ≥ 0.5). Further, these phytomolecules did not show any excessive bioaccumulation. mutagenicity and toxicity, thus making the respective phytoligands probable lead molecules [43]. All the selected, non-toxic druggable phytomolecules were then subjected to molecular docking with the target viral proteins.

In the present study, it was found that gamma-glutamyl-S-allylcysteine (Herbal source: *Allium sativum*, Garlic) irreversibly fits into the binding pockets of the target viral proteins utilizing forming electrostatic or hydrogen bonds with the glutamine amino acid residues of viral spike glycoprotein; glutamic acid residues of viral endoribonuclease; and proline amino acid of viral main protease. It has also been found that mutation or any change in the glutamine (508 aa position) or glutamic acid residues (528 aa position) of the Ebola virus spike glycoprotein causes viral neutralization. In particular, a specific change in the amino acid sequence at position 508 or 528 of the viral spike glycoprotein causes its neutralization [44]. Similarly, the proline amino acid residues (129 aa position) found in the conserved domains of HIV viral infectivity factor (VIF) are therapeutic targets for neutralizing the human immunodeficiency virus [45]. In a similar way, gamma-glutamyl-S-allylcysteine can bind to the glutamine residue (1071 aa position, located in the spacer/linker region between the HR1 and HR2 domains of the S2 subunit which is involved in viral fusion and entry. Hence, the irreversible binding of gamma-glutamyl-S-allylcysteine to glutamine, glutamic acid, and proline amino acid residues could cause the inactivation of the spike glycoprotein receptor, thereby ultimately leading to the inactivation of the SARS-CoV-2 virus.

Kubota & coworkers have suggested that gamma glutamyl cysteine ester derivatives could inhibit the HIV-1 gene transcription, wherein, it probably restrained the oxygen-free radical-mediated activation of the nuclear factor-kappa B21 [46]. Several other studies have also indicated that Sulphur compounds such as gamma-glutamyl-S-allylcysteine serves as redox modulators as well as selective inducers of cell death, and hence may also cause viral cell attenuation. In particular, S-allylcysteine inhibited the proliferation of A2780 cells

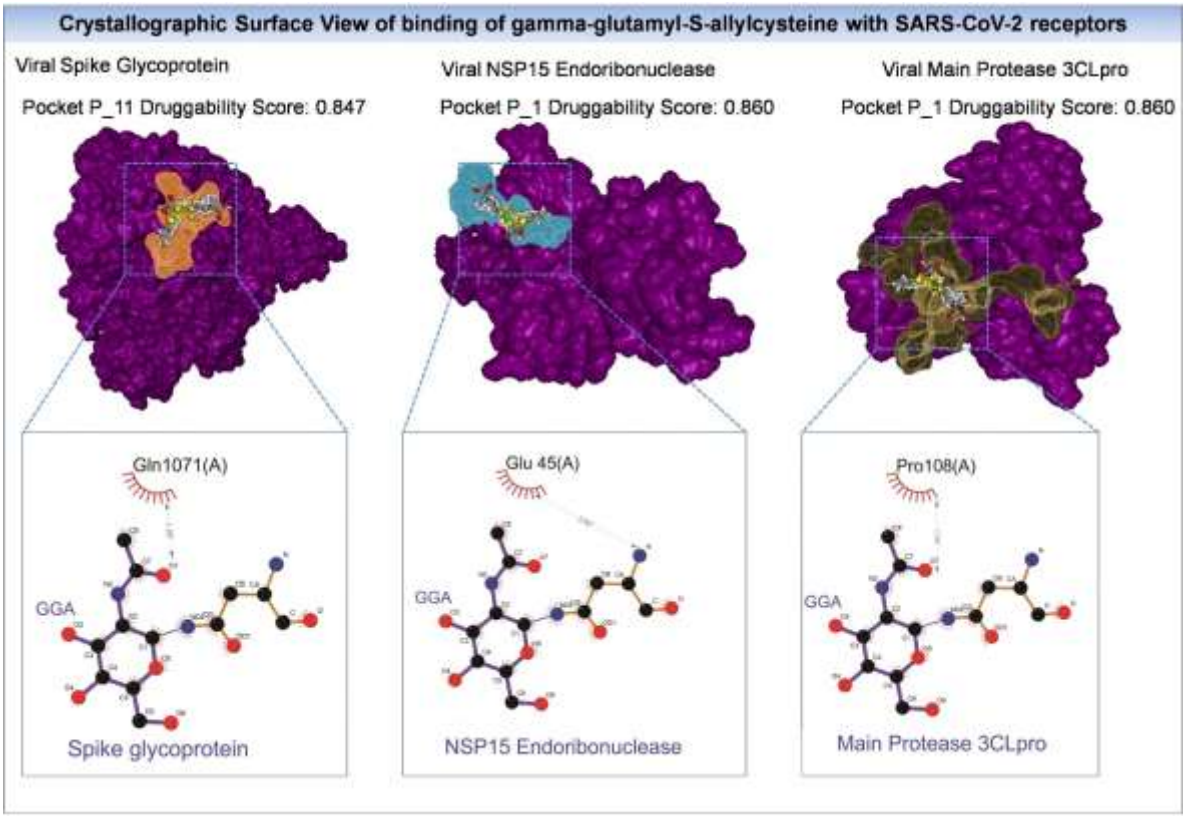

Fig. 3. Binding pose depictions of gamma-glutamyl-S-allylcysteine as probable drug candidate targeting SARS-CoV-2 receptors.

Amide group of gamma-glutamyl-S-allylcysteine (GGA) formed a hydrogen bond with the amide residue of glutamine amino acid (1071st position) of the viral spike glycoprotein. Glutamic acid residues (45th position) of viral endoribonuclease showed irreversible interaction with GGA. Additionally, the hydroxyl group of GGA formed a hydrogen bond with the carbonyl group of proline amino acid (108th position) of viral main protease 3CLpro.

(Human epithelial ovarian cancer cell line) and metastatic HCC cell line MHCC97L (hepatocellular carcinoma) in dose- and time-dependent manners [47, 48, 49]. It has been postulated that the apoptotic mechanism by which gamma-glutamyl-S-allylcysteine inhibits the progression of various cancer cell lines, in a similar manner it will be probably acting upon SARS-CoV-2. It has also been observed that bioactive compounds such as gamma-glutamyl-S-allylcysteine found in Garlic mainly affects the oxidative stress response mechanism, thereby imparting antiviral activity [20].

In a similar context, the present study also indicated that gamma-glutamyl-S-allylcysteine may contingently inhibit the entry of SARS-CoV-2 and also inactivate the viral protease as well as endoribonuclease, thereby inhibiting the process of viral capsid formation and replication altogether. Moreover, this moiety has a longer plasma life, bioavailability, and membrane permeability as compared to other tested herbal moieties, thereby making it a suitable drug candidate with sustained antiviral action [46]. The efficient binding energy of gamma-glutamyl-S-allylcysteine with all the target viral proteins further indicated it to be comparable with that of hydroxychloroquine which has been proposed as one of the possible treatments for COVID-19 therapy. However, recent clinical studies have suggested that hydroxychloroquine doesn't ameliorate the COVID-19 viral load and hence, is not effective in treating SARS-CoV-2 infection in most of the cases [50]. Several drugs are in various phases of trials and are being clinically tested against SARS-CoV-2. Recently, a combination of the drugs baricitinib and

remdesivir have been found as a combination therapy for COVID-19. However, upon extended continuation of the said combination therapy, in few cases venous thromboembolism has also been seen [51]. In such cases, herbal moeities such as gamma-glutamyl-S-allylcysteine could further be used as a safe herbal adjuvant for ameliorating the efficacy of hydroxychloroquine and other related chemosynthetic drugs. Gamma-glutamyl-S-allylcysteine has been considered safe for usage as it is 30-fold less toxic than other garlic compounds including allicin and diallyldisulfide. Although these herbal moieties have extensively been used for several years, however, before their clinical usage, it is imperative to evaluate their detailed safety and efficacy [52]. Future studies include detailed efficacy studies at *ex vivo* level by using cell lines such as Vero E6. Moreover, mechanistic assays (viral entry & attachment inhibition assay, viral protein expression measurement, and replication extent determination assay) will also be conducted in the near future to elucidate the mechanism of action of gamma-glutamyl-S-allylcysteine.

5. Conclusion

The novel Coronavirus infection accounts for innumerable deaths worldwide, and there is yet no absolute vaccine or treatment available. Global regulatory authorities have recently authorized the use of three COVID-19 vaccines. However, none of these vaccines have yet received complete authorization for global usage. Moreover, availability of a vaccine doesn't negate the need for therapeutics. Based on evidence from laboratory, animal, and clinical studies, Hydroxychloroquine is also one of the treatment options selected in 'Solidarity'- an international clinical trial to help find an effective treatment for COVID-19, launched by the World Health Organization and partners. However, the repurposed drug, hydroxychloroquine may cause adverse drug reactions and contraindications including cardiomyopathy, fulminant hepatic failure, vertigo, and other allergic reactions. Under such circumstances, there is an urgent need for screening novel natural leads that exhibit specific antiviral activities against SARS-CoV-2. The present study suggested that phytoligands derived from medicinal herbs exhibited potential binding properties toward major SARS-CoV-2 virulence factors. Selected phytomolecules were further screened based on acceptable pharmacokinetics and drug-like properties, thereby making them safely exploitable for the Coronavirus mitigation system. The current study showed that gamma-glutamyl-S-allylcysteine (GGA) specifically exhibited the most significant binding energy and docking pose toward the major viral virulence factors (E value $_{GGA + spike\ glycoprotein}$ = -578.57 Kcal/mol; E value $_{GGA + viral\ main\ protease}$ = -493.53 Kcal/mol; E value $_{GGA + endoribonuclease}$ = -825.00 Kcal/mol) in comparison with the known chemical moiety hydroxychloroquine (E value $_{HCQ + spike\ glycoprotein}$ = -207.47 Kcal/mol; E value $_{HCQ + viral\ main\ protease}$ = -235.48 Kcal/mol; E value $_{HCQ + endoribonuclease}$ = -213.54 Kcal/mol). Hence, the current study provides implications for the possible usage of gamma-glutamyl-S-allylcysteine (Herbal source: *Allium sativum*) as a novel and prospective drug candidate. This phytomolecule is also found in other species of the *Allium* genus (*A. cepa* and *A. schoenoprasum*). In view of the current viral pandemic and dearth of effective therapy, further studies should be urgently undertaken to explore the therapeutic potential of gamma-glutamyl-S-allylcysteine against SARS-CoV-2.

Author Contributions: "Conceptualization, A.B. and R.K.S.; methodology, P.T.; data curation, A.T., S.S.; writing—original draft preparation, P.T., A.T., S.S.; writing—review and editing, P.T.; supervision, R.K.S., N.S.; project administration, A.B. All authors have read and agreed to the published version of the manuscript."

Funding: "This research received no external funding".

Acknowledgments: The authors are grateful to Swami Ramdev Ji for institutional research facilities and supports. Authors gratefully acknowledge the efforts of colleagues of Patanjali Research Institute for their help in data collection and processing.

Conflicts of Interest: "The authors declare no conflict of interest."

References

1. Lefkowitz, E.J., Dempsey, D.M., Hendrickson, R.C., Orton, R.J., Siddell, S.G., Smith, D.B. Virus taxonomy: the database of the International Committee on Taxonomy of Viruses (ICTV). *Nucl Acids Res*, **2018**. *46*, D708-17. https://doi.org/10.1093/nar/gkx932 PMid:29040670 PMCid: PMC5753373
2. Hu, Z., Yang, Z., Li, Q., Zhang, A., Huang, Y. Infodemiological study on COVID-19 epidemic and COVID-19 infodemic. *Preprints* (Preprint). In press **2020**. Availablefrom: https://www.preprints.org/manuscript/202002.0380/v2 https://doi.org/10.2196/preprints.19135
3. Cucinotta, D., Vanelli, M. WHO declares COVID-19 a pandemic. *Acta Biomed: Atenei Parmensis* **2020**, 91, 157-60.
4. World Health Organization WHO: Rolling updates on Coronavirus disease- COVID 19 [database on the Internet]. Available online: https://www.who.int/emergencies/diseases/novel-coronavirus-2019/events-as-they-happen (accessed on 13 June 2020).
5. Balkrishna, A., Thakur, P., Singh, S., Dev, S., Jain, V., Varshney, A., et al. Glucose antimetabolite 2-Deoxy-D-Glucose and its derivative as promising candidates for tackling COVID-19: Insights derived from in silico docking and molecular simulations. *Authorea* (Preprint). In press **2020**. Available online: doi.org/10.22541/au.158567174.40895611
6. Our World in Data: Coronavirus Disease (COVID-19)-Statistics and Research [database on the Internet]. Roser M, Ritchie H, Ortiz-Ospina E. c **2020**. Available online: https://ourworldindata.org/coronavirus
7. Carlos, W.G., Dela Cruz, C.S., Cao, B., Pasnick, S., Jamil, S. Novel Wuhan (2019-nCoV) coronavirus. *Am J Respir Crit Care Med* **2020**, *201*, P7-8. https://doi.org/10.1164/rccm.2014P7 PMid:32004066
8. Yeo, C., Kaushal, S., Yeo, D. Enteric involvement of coronaviruses: is faecal-oral transmission of SARS-CoV-2 possible? *Lancet Gastroenterol Hepatol* **2020**, *5*, 335-7. https://doi.org/10.1016/S2468-1253(20)30048-0
9. Chen, N., Zhou, M., Dong, X., Qu, J., Gong, F., Han, Y., et al. Epidemiological and clinical characteristics of 99 cases of 2019 novel coronavirus pneumonia in Wuhan, China: a descriptive study. *The Lancet* **2020**, *395*, 507-13. https://doi.org/10.1016/S0140-6736(20)30211-7
10. Guo, Y.R., Cao, Q.D., Hong, Z.S., Tan, Y.Y., Chen, S.D., Jin, H.J., et al. The origin, transmission and clinical therapies on coronavirus disease 2019 (COVID-19) outbreak-an update on the status. *Mil Med Res* **2020**, *7*, 1-10. https://doi.org/10.1186/s40779-020-00240-0 PMid:32169119 PMCid: PMC7068984

11. Senathilake, K.S., Samarakoon, S.R., Tennekoon, K.H. Virtual screening of inhibitors against spike glycoprotein of SARS-CoV-2: a drug repurposing approach. *Preprints* (Preprint). In press **2020**. Available online: https://www.preprints.org/manuscript/202003.0042/v2 PMCid: PMC7370249
12. Wang, M., Li, M., Ren, R., Brave, A., van der Werf, S., Chen, E.Q., et al. International expansion of a novel SARS-CoV-2 mutant. *medRxiv* (Preprint). In press **2020**. Available from: https://www.medrxiv.org/content/10.1101/2020.03.15.20035204v1
13. Swargiary, A., Mahmud, S., & Saleh, M. A. Screening of phytochemicals as potent inhibitor of 3-chymotrypsin and papain-like proteases of SARS-CoV2: an in silico approach to combat COVID-19. *J Biomol Struct Dyn* **2020**, *38*, 1-15. https://doi.org/10.1080/07391102.2020.1835729
14. Chikhale, R. V., Sinha, S. K., Patil, R. B., Prasad, S. K., Shakya, A., Gurav, N., ... & Gurav, S. S. In-silico investigation of phytochemicals from Asparagus racemosus as plausible antiviral agent in COVID-19. *J Biomol Struct Dyn* **2020**, *38*, 1-15. doi: 10.1080/07391102.2020.1784289
15. Seshu, V., & Sahoo Suban, K. In silico admet and molecular docking study o n searching potential inhibitors from limonoids and triterpenoids for covid-19. *arXiv preprint* **2020**, arXiv:2005.07955. https://doi.org/10.1016/j.compbiomed.2020.103936 PMid: 32738628 PMCID: PMC7386496
16. Basu, A., Sarkar, A., & Maulik, U. Molecular docking study of potential phytochemicals and their effects on the complex of SARS-CoV2 spike protein and human ACE2. *Sci Rep* **2020**, *10*(1), 1-15. https://doi.org/10.1038/s41598-020-74715-4 PMid: 33077836 PMCID: PMC7573581
17. Tanwar, A., Zaidi, A. A., Kaur, H., Rana, N., Chawla, R., Basu, M., Arora, R., Khan, H. A. In silico bioprospection analysis for identification of herbal compound targeting Clostridium difficile. Indian J Tradit Knowl **2019**, *18*(4):655-61. doi:http://nopr.niscair.res.in/handle/123456789/50643
18. Harika, M.S., Renukadevi, V., Bhargavi, S., Karishma, S., Abbinaya, L., Ramya, L., et al. Virtual Screening Identifies New Scaffolds for Testosterone 17β-Dehydrogenase (NADP+) Inhibitor. *J Chem Pharm Res* **2017**, *9*, 134-8.
19. Park, K. J., & Lee, H. H. In vitro antiviral activity of aqueous extracts from Korean medicinal plants against influenza virus type A. *J Microbiol Biotechn* **2005**, *15*(5), 924-929.
20. Sharma, N. Efficacy of Garlic and Onion against virus. *Int J Res Pharm Sci* **2019**, *10*(4), 3578-3586.
21. Gautam, M., Diwanay, S., Gairola, S., Shinde, Y., Patki, P., & Patwardhan, B. Immunoadjuvant potential of Asparagus racemosus aqueous extract in experimental system. *J Ethnopharmacol* **2004**, *91*(2-3), 251-255. DOI: 10.1016/j.jep.2003.12.023
22. Chang, J. M., Kam, K. H., Chao, W. Y., Zhao, P. W., Chen, S. H., Chung, H. C., ... & Lee, Y. R. Berberine Derivatives Suppress Cellular Proliferation and Tumorigenesis In Vitro in Human Non-Small-Cell Lung Cancer Cells. *Int J Mol*

Sci **2020**, *21*(12), 4218-4230. doi: 10.3390/ijms21124218.

23. von Rhein, C., Weidner, T., Henß, L., Martin, J., Weber, C., Sliva, K., & Schnierle, B. S. Curcumin and Boswellia serrata gum resin extract inhibit chikungunya and vesicular stomatitis virus infections in vitro. *Antivir Res* **2016**, *125*, 51-57.
24. Ciesek, S., von Hahn, T., Colpitts, C. C., Schang, L. M., Friesland, M., Steinmann, J., ... & Pietschmann, T. The green tea polyphenol, epigallocatechin-3-gallate, inhibits hepatitis C virus entry. *Hepatology* **2011**, *54*(6), 1947-1955. DOI: 10.1002/hep.24610
25. Goel, A., Singh, R., Dash, S., Gupta, D., Pillai, A., Yadav, S. K., & Bhatia, A. K. Antiviral activity of few selected indigenous plants against Bovine Herpes Virus-1. *J Immunol Immunopathol* **2011**, *13*(1), 30-37.
26. Ma, H., He, X., Yang, Y., Li, M., Hao, D., & Jia, Z. The genus Epimedium: an ethnopharmacological and phytochemical review. *J Ethnopharmacol* **2011**, 134(3), 519-541. doi: 10.1016/j.jep.2011.01.001
27. Zou, W., Kim, B. O., Zhou, B. Y., Liu, Y., Messing, A., & He, J. J. (2007). Protection against human immunodeficiency virus type 1 Tat neurotoxicity by Ginkgo biloba extract EGb 761 involving glial fibrillary acidic protein. *Amer J Pathol* **2007**, *171*(6), 1923-1935. DOI: 10.2353/ajpath.2007.070333
28. Chiow, K. H., Phoon, M. C., Putti, T., Tan, B. K., & Chow, V. T. Evaluation of antiviral activities of Houttuynia cordata Thunb. extract, quercetin, quercetrin and cinanserin on murine coronavirus and dengue virus infection. *Asian Pac J Trop Med* **2016**, *9*(1), 1-7. DOI: 10.1016/j.apjtm.2015.12.002
29. Ibragić, S., Salihović, M., Tahirović, I., & Toromanović, J. Quantification of some phenolic acids in the leaves of Melissa officinalis L. from Turkey and Bosnia. *Bull Chem Tech Bosnia Herzegovina* **2014**, *42*, 47-50.
30. Sonar, V. P., Corona, A., Distinto, S., Maccioni, E., Meleddu, R., Fois, B., ... & Cottiglia, F. Natural product-inspired esters and amides of ferulic and caffeic acid as dual inhibitors of HIV-1 reverse transcriptase. *Eur J Med Chem* **2017**, *130*, 248-260.
31. Ho, J. Y., Chang, H. W., Lin, C. F., Liu, C. J., Hsieh, C. F., & Horng, J. T. Characterization of the anti-influenza activity of the Chinese herbal plant Paeonia lactiflora. *Viruses* **2014**, *6*(4), 1861-1875. doi: 10.3390/v6041861
32. Lee, N. Y., Khoo, W. K., Adnan, M. A., Mahalingam, T. P., Fernandez, A. R., & Jeevaratnam, K. The pharmacological potential of Phyllanthus niruri. *J Pharm Pharmacol* **2016**, *68*(8), 953-969. doi: 10.1111/jphp.12565.
33. Zakaryan, H., Arabyan, E., Oo, A., & Zandi, K. Flavonoids: promising natural compounds against viral infections. *Arch Virol* **2017**, *162*(9), 2539-2551.
34. Abd-Elazem, I. S., Chen, H. S., Bates, R. B., & Huang, R. C. C. (2002). Isolation of two highly potent and non-toxic inhibitors of human immunodeficiency virus type 1 (HIV-1) integrase from Salvia miltiorrhiza. *Antivir Res*, *55*(1),

91-106.doi:10.1016/s0166-3542(02)00011-6.

35. Yang, L., Lin, J., Zhou, B., Liu, Y., & Zhu, B. Activity of compounds from Taxillus sutchuenensis as inhibitors of HCV NS3 serine protease. *Nat Prod Res* **2017**, *31*(4), 487-491.
36. Rege, A. A., Ambaye, R. Y., & Deshmukh, R. A. In vitro testing of anti-HIV activity of some medicinal plants. *Indian J Nat Prod Resour* **2010**, *1*(2), 193-199.
37. Shree, P., Mishra, P., Selvaraj, C., Singh, S. K., Chaube, R., Garg, N., & Tripathi, Y. B. Targeting COVID-19 (SARS-CoV-2) main protease through active phytochemicals of ayurvedic medicinal plants–Withania somnifera (Ashwagandha), Tinospora cordifolia (Giloy) and Ocimum sanctum (Tulsi)–a molecular docking study. *J Biomol Struct Dyn* **2020**, *27*, 1-14. DOI: 10.1080/07391102.2020.1810778
38. Dissanayake, K. G. C., Waliwita, W. A. L. C., & Liyanage, R. P. A review on medicinal uses of Zingiber officinale (Ginger). *Int J Health Sci Res* **2020**, *6*(7), 142-148.
39. Anand, K., Ziebuhr, J., Wadhwani, P., Mesters, J. R., Hilgenfeld, R. Coronavirus main proteinase (3CLpro) structure: basis for design of anti-SARS drugs. *Science* **2003**, *300*, 1763-67. doi: https://doi.org/10.1126/science.1085658 PMid:12746549
40. Kumar, R., Kumar, S., Sangwan, S., Yadav, I.S., Yadav, R. Protein modeling and active site binding mode interactions of myrosinase-sinigrin in Brassica juncea-An in-silico approach. *J Mol Graph Model* **2011**, *29*, 740-6. https://doi.org/10.1016/j.jmgm.2010.12.004 PMid:21236711
41. Volkamer, A., Kuhn, D., Rippmann, F., Rarey, M. DoGSiteScorer: a web server for automatic binding site prediction, analysis and druggability assessment. *Bioinformatics* **2012**, *28*, 2074-5. https://doi.org/10.1093/bioinformatics/bts310 PMid:22628523
42. Zhang, M.Q., Wilkinson, B. Drug discovery beyond the 'rule-of-five'. *Curr Opin Biotechnol* **2007**, *18*, 478-88. https://doi.org/10.1016/j.copbio.2007.10.005 PMid:18035532
43. Nisha, C.M., Kumar, A., Vimal, A., Bai, B.M., Pal, D., Kumar, A. Docking and ADMET prediction of few GSK-3 inhibitors divulges 6-bromoindirubin-3-oxime as a potential inhibitor. *J Mol Graph Model* **2016**, *65*, 100-7. https://doi.org/10.1016/j.jmgm.2016.03.001 PMid:26967552
44. Reynard, O., Volchkov, V.E. Characterization of a novel neutralizing monoclonal antibody against Ebola virus GP. *J Infect Dis* **2015**, *212*, S372-8. https://doi.org/10.1093/infdis/jiv303 PMid:26232760
45. Ralph, R., Lew, J., Zeng, T., Francis, M., Xue, B., Roux, M., et al. 2019-nCoV (Wuhan virus), a novel Coronavirus: human-to-human transmission, travel-related cases, and vaccine readiness. *J Infect Dev Ctries* **2020**, *14*, 3-17. https://doi.org/10.3855/jidc.12425 PMid:32088679
46. Kubota, S., Shetty, S., Zhang, H., Kitahara, S., Pomerantz, R.J. Novel inhibitory effects of γ-glutamylcysteine ethyl ester against human immunodeficiency virus type 1 production and propagation. *Antimicrob Agents Chemother* **1998**, *42*,1200-6.

https://doi.org/10.1128/AAC.42.5.1200 PMid:9593150 PMCid: PMC105777

47. Ng, K. T., Guo, D. Y., Cheng, Q., Geng, W., Ling, C. C., Li, C. X., ... & Fan, S. T. A garlic derivative, S-allylcysteine (SAC), suppresses proliferation and metastasis of hepatocellular carcinoma. *PLoS One* **2012**, *7*(2), e31655. DOI: 10.1371/journal.pone.0031655
48. Liu, Z., Li, M., Chen, K., Yang, J., Chen, R., Wang, T., ... & Ye, Z. S-allylcysteine induces cell cycle arrest and apoptosis in androgen-independent human prostate cancer cells. *Mol Med Rep* **2012**, *5*(2), 439-443. DOI: 10.3892/mmr.2011.658
49. Agbana, Y. L., Ni, Y., Zhou, M., Zhang, Q., Kassegne, K., Karou, S. D., ... & Zhu, Y. Garlic-derived bioactive compound S-allylcysteine inhibits cancer progression through diverse molecular mechanisms. *Nutr Res* **2020**, *73*, 1-14.
50. Funnell, S. G. P., Dowling, W. E., Muñoz-Fontela, C., Gsell, P. S., Ingber, D. E., Hamilton, G. A., ... & Neyts, J. Emerging preclinical evidence does not support broad use of hydroxychloroquine in COVID-19 patients. *Nature Commun* **2020**, *11*(1), 1-4. https://doi.org/10.1038/s41467-020-17907-w PMid: 32848158
51. Kalil, A. C., Patterson, T. F., Mehta, A. K., Tomashek, K. M., Wolfe, C. R., Ghazaryan, V., ... & Tapson, V. Baricitinib plus Remdesivir for Hospitalized Adults with Covid-19. *N Engl J Med* **2020**, *383*(24), 1-13. https://doi.org/10.1056/NEJMoa2031994 PMid: 33306283
52. Colín-González, A. L., Santana, R. A., Silva-Islas, C. A., Chánez-Cárdenas, M. E., Santamaría, A., & Maldonado, P. D. The antioxidant mechanisms underlying the aged garlic extract-and S-allylcysteine-induced protection. *Oxid Med Cell Longev* **2012**, 1-16. https://doi.org/10.1155/2012/907162 PMid: 22685624 PMCID: PMC3363007